OPEN ACCESS

Applied Physics Express **11**, 063007 (2018)

https://doi.org/10.7567/APEX.11.063007

Néel skyrmion stability in ultrathin circular magnetic nanodots

Konstantin Y. Guslienko[1,2*]

[1]Departamento de Física de Materiales, Universidad del País Vasco, UPV/EHU, 20018 San Sebastian, Spain
[2]IKERBASQUE, The Basque Foundation for Science, 48013 Bilbao, Spain

*E-mail: kostyantyn.gusliyenko@ehu.eus

Received April 21, 2018; accepted May 10, 2018; published online May 25, 2018

The stability of Néel skyrmions in ultrathin circular magnetic nanodots is calculated by considering the Dzyaloshinskii–Moriya exchange interaction (DMI) as an interface term. The areas of the single-Néel skyrmion stability/metastability/instability and skyrmion radius are determined as functions of the uniaxial out-of-plane magnetic anisotropy and DMI strength. It is shown that the well-known criterion of skyrmion stability in infinite film should be changed to describe the stability in nanodots. Néel skyrmions can be the ground state for dots of finite radius, whereas they can only be metastable in infinite films. The skyrmion stability area is extended by decreasing the out-of-plane anisotropy.

Magnetic skyrmions — inhomogeneous topologically non-trivial magnetization textures on the nanoscale — are a type of magnetic topological solitons[1] in two-dimensional (2D) spin systems characterized by a non-zero skyrmion number (topological charge), which is defined as $N = \int d^2\boldsymbol{\rho}\mathbf{m} \cdot (\partial_x \mathbf{m} \times \partial_y \mathbf{m})/4\pi$, where $\mathbf{m}(\boldsymbol{\rho}) = \mathbf{M}(\boldsymbol{\rho})/M_s$ is the unit magnetization vector, M_s is the saturation magnetization, and $\boldsymbol{\rho} = (x, y)$ are in-plane spatial coordinates.

Individual magnetic skyrmions in a restricted geometry have attracted considerable attention from researchers owing to their potential applications in spintronic devices, because the skyrmion motion can be controlled by an ultralow-density spin-polarized current.[2,3] To achieve efficient manipulation of nanosized spin textures and realize skyrmion-based low-energy consumption spintronic devices, it is essential to understand the magnetic skyrmion stability and dynamics in confined geometries, for instance, in ultrathin magnetic nanodots and stripes. The relativistic Dzyaloshinskii–Moriya exchange interaction (DMI), existing at the ferromagnetic metal and heavy metal interface in ultrathin films, leads to the stabilization of Néel skyrmions with a given sense of the magnetization rotation.[3,4] These individual chiral Néel skyrmions were recently observed at room temperature by Boulle et al. in Pt/Co/MgO,[5] Moreau-Luchaire et al. in Ir/Co/Pt,[6] Woo et al. in Pt/Co/Ta, Pt/CoFeB/MgO,[7] and Pollard et al. in Pd/Co[8] ultrathin multilayer films and dots.

The role of the DMI in skyrmion stabilization was discussed in Refs. 9–12. Following the ideas of Dzyaloshinskii,[9] it was found[10] that adding to the magnetic energy of an infinite cubic ferromagnet a term $D[\mathbf{m} \cdot (\nabla \times \mathbf{m})]$ linear in spatial derivatives of magnetization leads to the stabilization of an inhomogeneous magnetization texture for any finite value of D. Such terms are allowed in magnetic crystals whose symmetry group lacks the space inversion symmetry operation. Then, it was shown[11] that accounting for the DMI in the form of the Lifshitz invariants in a bulk uniaxial ferromagnet results in instability of the uniform ferromagnetic state at $D > D_c = (4/\pi)\sqrt{AK}$, where A is the exchange stiffness, and K is a uniaxial anisotropy constant. Therefore, the DMI can stabilize 2D Bloch skyrmions (in modern terminology). Ivanov et al.[12] showed that the Bloch skyrmions in infinite films with easy axis anisotropy can be stabilized by either DMI or a high-order exchange interaction. In the case of an infinite film, the critical D value remains $D_c^f = (4/\pi)\sqrt{AK}$, although the effective anisotropy constant K is different. The isolated skyrmions are metastable at $D < D_c^f$, and other configurations (skyrmion lattices, stripe domains) are stabilized at $D > D_c^f$. Presumably, some finite value of the interface DMI strength is necessary for stabilization of a single Néel skyrmion in ultrathin magnetic dots, similar to that needed for skyrmion stabilization in bulk uniaxial ferromagnets. The value of D_c^f can be used as a qualitative criterion to estimate the stability of 2D magnetic skyrmions in a restricted geometry, especially in thin dots.[4] The DMI reduces the skyrmion energy for the proper skyrmion chirality. Therefore, the skyrmion stability in a dot should increase with D, leading to a single skyrmion ground state at $D > D_c$, where the value of D_c should be defined. On the other side, large values of D lead to the stabilization of more complicated inhomogeneous states (multi-skyrmion, multi-domain, etc.).

In this study, we calculate the magnetic energy of a single Néel skyrmion in ultrathin cylindrical dots, determine the area of the skyrmion stability/metastability and the equilibrium skyrmion radius, and obtain the skyrmion magnetization profiles. The case of an effective out-of-plane magnetic anisotropy is analyzed. The dot magnetic parameters, including the DMI strength, are varied within reasonable ranges to draw conclusions about the stability/metastability/instability of the skyrmion configurations.

Let us consider a thin circular magnetic dot with radius R and thickness L [Fig. 1(a)] and parameterize the unit magnetization vector by the spherical angles, $\mathbf{m} = \mathbf{m}(\Theta, \Phi)$. The angles Θ, Φ are functions of the polar radius vector $\boldsymbol{\rho} = (\rho, \varphi)$ located in the dot plane. For this kind of the magnetization configuration, the total magnetic energy functional is $E[\mathbf{m}] = L\int d^2\boldsymbol{\rho}\,\varepsilon(\mathbf{m})$,[11,12] with the energy density

$$\varepsilon(\mathbf{m}) = A(\nabla\mathbf{m})^2 + \varepsilon_{DMI}(\mathbf{m}) - K_u m_z^2 + \varepsilon_m(\mathbf{m}), \tag{1}$$

where $\varepsilon_{DMI} = D[m_z(\nabla \cdot \mathbf{m}) - (\mathbf{m} \cdot \nabla)m_z]$ is the interface DMI energy density, with D being the DMI parameter, $K_u > 0$ is the out-of-plane uniaxial anisotropy constant, m_z is the magnetization z-component, and ε_m is the magnetostatic energy. The magnetostatic energy is non-local in the general case. However, within the limit of the ultrathin dot ($\beta = L/R \to 0$), the magnetostatic energy density can be simplified and written in the local form $\varepsilon_m(\mathbf{m}) = \mu_0 M_s^2 m_z^2/2$. Therefore, the

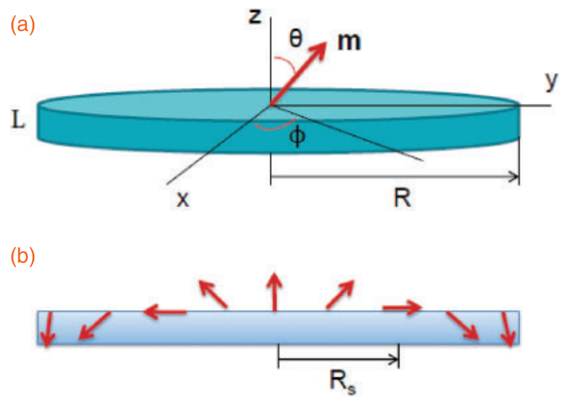

Fig. 1. Sketch of the cylindrical magnetic dot and the coordinate system used: (a) $\mathbf{m}(\Theta, \Phi)$ is the unit magnetization vector described by the spherical polar angle Θ and the azimuthal angle Φ; (b) Néel skyrmion magnetization distribution in the dot cross-section by the radial plane yz. The dot radius is R, and the skyrmion radius is R_s.

energy is accounted via an effective uniaxial anisotropy constant $K = K_u - \mu_0 M_s^2/2$. We also define the magnetic material quality factor as $Q = 2K_u/\mu_0 M_s^2$ and consider the case of $Q \geq 1$.

The magnetization is assumed to be independent of the thickness coordinate z. We search for axially symmetric magnetization configurations (**m** depends only on the radial coordinate ρ); i.e., the magnetization angles are $\Theta = \Theta(\rho)$ and $\Phi = \varphi + \varphi_0$ [$\varphi_0 = 0, \pi$ for the Néel skyrmions considered below, see Fig. 1(b)]. The skyrmion number for the radially symmetric skyrmions is $N = [\cos(\Theta(0)) - \cos(\Theta(R))]/2$. The total skyrmion magnetic energy as a functional of the skyrmion magnetization is represented by the polar magnetization angle $\Theta(\rho)$, $E = E[\Theta(\rho)]$. We can write the Lagrange–Euler equation for the function $\Theta(\rho)$ to minimize the skyrmion energy (1) using the substitution $\tan[\Theta(r)/2] = \exp[-f(r)]$:

$$f'' + \frac{1}{r}f' + \left[\left(\xi^2 + \frac{1}{r^2}\right) - (f')^2\right]\tanh(f) - \frac{d}{r}\frac{1}{\cosh(f)} = 0, \tag{2}$$

where $r = \rho/l_{ex}$, $\xi^2 = Q - 1$, the reduced DMI strength is $d = |D|l_{ex}/A$, and $l_{ex} = \sqrt{2A/\mu_0 M_s^2}$ is the exchange length.

The boundary conditions for the function $\Theta(\rho)$ are $\Theta(0) = \pi$ and $\Theta'_r(R) = d/2$.[13] Instead of the latter condition for ultrathin dots ($R/L \gg 1$), it is more convenient to use the condition $\Theta(R) = 0$, which is similar to that used for the description of the isolated skyrmions in infinite film. This is justified for large dot radii ($r_d = R/l_{ex} \gg 1$), where the edge area of the dot contributes negligibly to the dot magnetic energy. Such a boundary condition results in the integer skyrmion number $|N| = 1$. The boundary conditions for the function $f(r)$ are $f(0) = -\infty$ (exact) and $f(r_d) = \infty$ (approximate, $r_d \gg 1$). We define the skyrmion radius $R_s < R$ using the equation $m_z(R_s) = 0$, $\Theta(R_s) = \pi/2$ or $f(r_s) = 0$, where the reduced radius is $r_s = R_s/l_{ex}$.

The solution of Eq. (2) allows calculating the radially symmetric skyrmion energy as

$$E[\Theta(r)] = 2\pi AL\int_0^{r_d} dr\, r\left[(\Theta'_r)^2 + \left(\frac{1}{r^2} + \xi^2\right)\sin^2\Theta + d\left(\Theta'_r + \frac{1}{r}\sin\Theta\cos\Theta\right)\right] + E[0], \tag{3}$$

where $E[0] = \mu_0 M_s^2 V/2$ is the energy of the perpendicular single-domain state ($V = \pi R^2 L$ is the dot volume).

Equation (2) is a non-linear differential equation and cannot be, in general, solved analytically. For this reason, we use different approximate solutions or trial functions for the skyrmion magnetization profile, $\Theta(\rho)$. By introducing a trial function (skyrmion ansatz) to the energy functional (3), one can obtain the energy of the skyrmion configuration. It is evident that the solution of Eq. (2) depends on only two parameters: d and ξ. In the simplest case of an isotropic dot with $\xi = 0$, without DMI $d = 0$, the exact solution satisfying the boundary conditions is $f(r) = \ln(r/r_s)$, or the Belavin–Polyakov (BP) soliton.[14] The BP ansatz is also an approximate solution when $r \to 0$ for any ξ, d. The trial function proposed by Ezawa,[15] $f(r) = \xi r_s \ln(r/r_s)$ (a generalized BP ansatz with the effective topological charge $q = \xi r_s$), formally satisfies the boundary conditions but does not satisfy Eq. (2). The approximate solution of Eq. (2) at $r \gg 1$, which is far from the dot center $r = 0$, is $f(r) = \xi(r - r_s)$ or $\tan[\Theta(\rho)/2] = \exp[-(\rho - R_s)/\Delta]$, where $\Delta = \sqrt{A/K}$ is the domain-wall width. This is a frequently used radial domain-wall ansatz. This ansatz yields $f(0) = -\xi r_s$ and does not satisfy the exact boundary condition $f(0) = -\infty$, resulting in the singularity of the exchange energy at $r = 0$. It can be used with precaution only within the limit $\xi r_s = R_s/\Delta \gg 1$, i.e., for large-radius skyrmions, $Q > 1$, and thin domain walls. To avoid the singularity at $r = 0$ and describe all ranges of the skyrmion radii r_s, we use the trial function $f(r) = \ln(r/r_s) + \xi(r - r_s)$ suggested by DeBonte[16] to describe bubble domains in infinite films. Although this function is not a solution of Eq. (2), it is evident that $f(r)$ satisfies the boundary conditions and is reduced to the BP ansatz at $\xi = 0$ and to the domain-wall ansatz at $r \gg 1$.

We use below the ansatz $f(r) = \ln(r/r_s) + \xi(r - r_s)$, $\cos\Theta(r) = \tanh f(r)$, and $\sin\Theta(r) = 1/\cosh f(r)$ to calculate the skyrmion energy (3) and find the areas of the skyrmion metastability/stability. We consider that a skyrmion state is stable when it has the lowest energy (ground state) compared with the other magnetization states, and a skyrmion is metastable when its energy is higher than that of any of other magnetization configuration. The Néel skyrmion energy $E(r_s, \xi)$ is a function of two parameters: r_s and ξ (ξ^{-1} can be considered as the skyrmion radius in units of l_{ex}). However, it was shown numerically in Ref. 17 that for a fixed dot radius R and wide range of D ($0.5 < D/D_c < 2$) the parameter ξ^{-1} is almost constant and equal to its nominal value $\xi^{-1} = 1/\sqrt{Q-1}$. Considering $\Theta'_r = -(\xi + 1/r)\sin\Theta$, we rewrite the skyrmion energy as

$$E(r_s, \xi) = 2\pi AL\int_0^{r_d} dr\frac{r}{\cosh^2 f(r)}\left[2\left(\frac{1}{r^2} + \xi^2 + \frac{\xi}{r}\right) - d\left(\xi\cosh f(r) + \frac{e^{-f(r)}}{r}\right)\right] \tag{4}$$

and minimize it with respect to the skyrmion radius r_s using the standard procedure $\partial E/\partial r_s = 0$, $\partial^2 E/\partial r_s^2 \geq 0$. We plot the skyrmion-stability phase diagram in Fig. 2, applying the definition that skyrmions with the radius $R_s/R \to 0$ correspond to the perpendicular single-domain state $m_z(r) = +1$ (area marked by the symbol u), whereas skyrmions with the radius $R_s > R$ correspond to the single-domain state $m_z(r) \approx -1$ (area marked by the symbol u'). There is only one

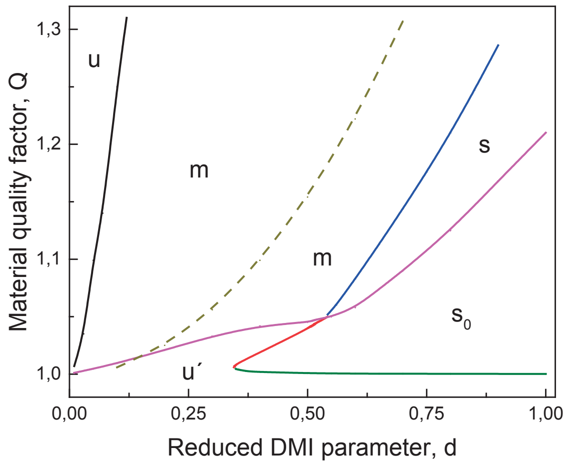

Fig. 2. Phase diagram of the Néel skyrmion stability in an ultrathin circular dot. The reduced dot radius is $R/l_{ex} = 20$. The skyrmion is the ground state of the dot in the areas s and s_0. $Q = 2K_u/\mu_0 M_s^2 \geq 1$ is the magnetic material quality factor, and $d = |D|l_{ex}/A$ is the reduced strength of the DMI. The dark yellow dashed line describes the critical line of the skyrmion metastability $d_c^f(Q) = (4/\pi)\sqrt{Q-1}$ calculated within the domain-wall model for an infinite film.[4]

minimum of the energy (4) in the areas u and u'. The areas marked by the symbols m and s describe bi-stability regions, where the skyrmion is metastable and the single-domain state is stable (m) and where the skyrmion is stable and single-domain state is metastable (s). Only the Néel skyrmion stable state exists in the area marked as s_0. The solid blue line corresponds to the equilibrium of the m- and s-states determined by the equation $E_s(Q, d) = E_{SD}(Q, d)$, at which the skyrmion energy is equal to the single-domain state energy.

The lines in the phase diagram (Fig. 2) are explained as follows. The black line describes the u–m boundary and is determined by the equation $r_s(Q, d) = 0$. The red–green line corresponds to the s_0–u' boundary and is determined by the equation $r_s(Q, d) = 1$ at small values of $Q - 1$. The pink line at large values of the DMI parameter d describes the s–s_0 boundary (the second large radius energy minimum moves outside the dot and disappears). The pink line at small values of d describes the m–u' boundary. The skyrmion metastable minimum disappears with decreasing Q, after which only the u' perpendicular single-domain state minimum exists.

As described above, we calculated the stability of the Néel skyrmion magnetization configurations in ultrathin circular dots with the interfacial DMI energy. The skyrmion state is metastable for the majority of the points in the Q–d space (Fig. 2). The Néel skyrmion is the ground state at $d > d_c(Q)$, where the function $d_c(Q)$ represented by blue, red, and green lines in Fig. 2 reveals a deep minimum at small values of Q ($d_{min} = 0.35$ for the given $R/l_{ex} = 20$). The skyrmions are metastable within a wide range of values of D satisfying the inequality $d < d_c(Q)$, except in regions of a small Q and small D (Fig. 2). Therefore, values of Q slightly above 1 are optimal for stabilizing the Néel skyrmion in an ultrathin circular magnetic dot for moderate values of d. The phase Q–d diagram plotted in Fig. 2 does not depend on the dot magnetic parameters (A, M_s, K_u, D). It depends weakly only on the reduced dot radius R/l_{ex}. The DMI is determined via the dimensionless combination $d \propto D/M_s\sqrt{A}$. The typical value of D accessible in experiments with ultrathin films and dots such as X/Co (X = Pt, Ir, Pd) is 1–2 mJ/m^2; therefore, moderate values of the dot magnetization M_s and the exchange stiffness A are necessary to obtain stable Néel skyrmions with $d = 0.5$–0.8.

To describe the skyrmion magnetization analytically, we used the DeBonte radial domain-wall ansatz,[16] whose accuracy was numerically checked for circular dots in Ref. 18. The calculated equilibrium skyrmion radius $R_c(D)$ increases with the increase of the DMI strength (Fig. 2) at a fixed value of Q. The skyrmion radius is always small at $D < D_c$ in the area of the skyrmion-state metastability (m). $R_c(D)$ increases sharply in the region of $D \approx D_c$ (m–s boundary) for all calculated dot radii and becomes saturated at a large D (in the s_0 area), reaching values of $R_c(D)/R \approx 0.6$–0.7 for any $Q > 1$ and typical dot radii of $R = 100$–200 nm. Qualitatively, this agrees well with the simulations reported by Rohart et al.[4] for small dot radii of $R \leq 100$ nm. However, the calculated values of $d_c(Q)$ are essentially larger than those calculated by Rohart et al. $d_c^f(Q) = (4/\pi)\sqrt{Q-1}$ for small values of Q and approach them at increasing Q. The condition $R_s/\Delta \gg 1$ is satisfied at $Q \gg 1$, and the domain-wall model becomes asymptotically exact. The Néel skyrmion is unstable for small D according to Fig. 2, whereas the skyrmion is metastable for all $D < D_c$ according to the domain-wall model[4] for a ultrathin circular dot or infinite film and according to the simulations[19] for an infinite film of finite thickness.

Many authors, including Rohart et al.[4] and Buettner et al.,[20] following the theory of bubble domains in infinite films,[21] considered the skyrmion magnetization configuration as a circular domain wall located at the skyrmion radius position R_s described by the singular ansatz $\tan[\Theta(\rho)/2] = \exp[\pm(\rho - R_s)/\Delta]$. The domain-wall model predicts the skyrmion radius $R_s(D)$ singularity at $D \to D_c - 0$ and no dependence of R_s on the dot radius R. Therefore, this model does not account for the difference between the infinite film and the finite dot. This seems to be non-realistic for magnetic dots having a finite R of approximately 100 nm and contradicts the micromagnetic simulations reported by Rohart et al.[4] yielding stable skyrmions at $D > D_c$. A more rigorous approach to the skyrmion stability developed in the present work involves searching for the skyrmion energy minima and comparing the skyrmion energy with the energy of the perpendicularly magnetized state ($Q > 1$) and other competing magnetization configurations (e.g., vortex or in-plane single domain) if $Q < 1$ (not considered here).

To the knowledge of the author, presently only two experimental papers are published on Néel skyrmion observations via X-ray imaging in square Pt/Co/MgO dots[5] and circular Ir/Co/Pt dots.[6] The magnetic parameters of the circular dots[6] are $M_s = 960$ kA/m, $A = 15$ pJ/m or $l_{ex} = 5.1$ nm, and $Q \approx 1.30$. Using the value of $D = 1.4$–1.6 mJ/m,[2,6] we obtain the reduced DMI strength $d = 0.46$–0.53. Néel skyrmions with such parameters are metastable according to the phase diagram plotted in Fig. 2. The strong dependence of the skyrmion radius on the out-of-plane magnetic field and relatively small values of the reduced radius $R_s/R \approx 0.1$–0.2 measured in Ref. 6 indirectly support the conclusion regarding the skyrmion metastability.

In the investigated case of out-of-plane effective magnetic anistropy $Q > 1$, the large values of the DMI D cause the nucleation of more complicated magnetization configurations

($n\pi$-skyrmions,[4] labyrinth domain, etc.); i.e., the individual Néel skyrmion state with the topological charge $|N| \approx 1$ is no longer metastable or stable. This is beyond the scope of the present article, where only the values of the reduced DMI parameter $d < 1$ are considered.

In summary, the value of the material quality parameter $Q = 2K/\mu_0 M_s^2$ defining the effective out-of-plane dot magnetic anisotropy is important for Néel skyrmion stabilization, along with the DMI strength D. Almost all calculated Néel skyrmions in ultrathin circular nanodots are metastable. The skyrmion stability area is relatively small in terms of the dot magnetic parameters d and Q. The skyrmions are metastable if the DMI strength is $D < D_c(Q)$, where D_c is the DMI critical value, and stable (the nanodot ground state) if $D > D_c(Q)$. The function $D_c(Q)$ has a deep minimum at $Q \approx 1$ that allows optimizing the ultrathin dot magnetic parameters to stabilize the Néel skyrmions.

Acknowledgments The author thanks A. N. Bogdanov for the discussion on the general properties of chiral magnetic skyrmions. The author acknowledges support by IKERBASQUE (The Basque Foundation for Science). The work was partially supported by the Spanish MINECO grant FIS2016-78591-C3-3-R and the European Union's Horizon 2020 research and innovation programme under the Marie Skłodowska-Curie grant agreement No. 644348.

1) A. M. Kosevich, B. A. Ivanov, and A. A. Kovalev, Phys. Rep. **194**, 117 (1990).
2) A. Fert, V. Cros, and J. Sampaio, Nat. Nanotechnol. **8**, 152 (2013).
3) J. Sampaio, V. Cros, S. Rohart, A. Thiaville, and A. Fert, Nat. Nanotechnol. **8**, 839 (2013).
4) S. Rohart and A. Thiaville, Phys. Rev. B **88**, 184422 (2013).
5) O. Boulle, J. Vogel, H. Yang, S. Pizzini, D. S. Chaves, A. Locatelli, T. O. Mentes, A. Sala, L. D. Buda-Prejbeanu, O. Klein, M. Belmeguenai, Y. Roussigne, A. Stashkevich, S. M. Cherif, L. Aballe, M. Foerster, M. Chshiev, S. Auffret, I. M. Miron, and G. Gaudin, Nat. Nanotechnol. **11**, 449 (2016).
6) C. Moreau-Luchaire, C. Moutafis, N. Reyren, J. Sampaio, C. A. F. Vaz, N. Van Horne, K. Bouzehouane, K. Garcia, C. Deranlot, P. Warnicke, P. Wohlhüter, J.-M. George, M. Weigand, J. Raabe, V. Cros, and A. Fert, Nat. Nanotechnol. **11**, 444 (2016).
7) S. Woo, K. Litzius, B. Krüger, M.-Y. Im, L. Caretta, K. Richter, M. Mann, A. Krone, R. M. Reeve, M. Weigand, P. Agrawal, I. Lemesh, M.-A. Mawass, P. Fischer, M. Kläui, and G. S. D. Beach, Nat. Mater. **15**, 501 (2016).
8) S. D. Pollard, J. A. Garlow, J. Yu, Z. Wang, Y. Zhu, and H. Yang, Nat. Commun. **8**, 14761 (2017).
9) I. E. Dzyaloshinskii, Sov. Phys. JETP **19**, 960 (1964).
10) P. Bak and M. H. Jensen, J. Phys. C **13**, L881 (1980).
11) A. N. Bogdanov and D. A. Yablonskii, Sov. Phys. JETP **95**, 178 (1989).
12) B. A. Ivanov, V. A. Stephanovich, and A. A. Zhmudskii, J. Magn. Magn. Mater. **88**, 116 (1990).
13) H. Du, W. Ning, M. Tian, and Y. Zhang, Europhys. Lett. **101**, 37001 (2013).
14) A. A. Belavin and A. M. Polyakov, JETP Lett. **22**, 245 (1975).
15) M. Ezawa, Phys. Rev. Lett. **105**, 197202 (2010).
16) W. J. DeBonte, J. Appl. Phys. **44**, 1793 (1973).
17) A. R. Aranda, A. Hierro-Rodriguez, G. N. Kakazei, O. Chubykalo-Fesenko, and K. Y. Guslienko, submitted to J. Magn. Magn. Mater. (2018).
18) R. Tomasello, K. Y. Guslienko, M. Ricci, A. Giordano, J. Barker, M. Carpentieri, O. Chubykalo-Fesenko, and G. Finocchio, Phys. Rev. B **97**, 060402 (2018).
19) N. S. Kiselev, A. N. Bogdanov, R. Schaefer, and U. K. Roessler, J. Phys. D **44**, 392001 (2011).
20) F. Büttner, I. Lemesh, and G. S. D. Beach, Sci. Rep. **8**, 4464 (2018).
21) A. P. Malozemoff and J. C. Slonczewski, *Magnetic Domain Walls in Bubble Materials* (Academic Press, New York, 1979).